

Noncovalent Self-Assembly of Silver Nanocrystal Aggregates in Solution

Stephen Fullam, S. Nagaraja Rao, and Donald Fitzmaurice*

Department of Chemistry, University College Dublin, Belfield, Dublin 4, Ireland

Received: February 17, 2000

Size monodisperse silver nanocrystals have been stabilized by chemisorption of long-chain alkane thiols incorporating a receptor site. When dispersed in a suitable solvent these nanocrystals recognize and selectively bind a long-chain alkane incorporating two complementary substrate sites and are noncovalently linked. The nanocrystal aggregates formed as a result have been studied by NMR, FT-IR, and dynamic light scattering. As a consequence, it has been possible to characterize the interactions between the receptor and substrate sites that lead to nanocrystal aggregation. It has also been possible to gain insights into the factors that affect the size, shape, and internal structure of the nanocrystal aggregates formed. An important insight is that the kinetics of nanocrystal aggregation, and as a consequence the structure of the nanocrystal aggregates formed, depends on the number of receptor sites at the surface of a nanocrystal.

Introduction

The size-dependent properties of nanocrystals have been studied in detail.^{1–9} Increasingly, however, it is the collective properties of organized assemblies of nanocrystals that are being studied.^{3,10,11} These studies are being facilitated in large part by the preparation of superlattices of size-monodisperse nanocrystals.^{1,5,10–14} Of particular interest is how the size-dependent electronic and magnetic properties of the constituent nanocrystals can be exploited to tune their collective properties.

Generally, nanocrystal superlattices are prepared at an air–water interface using Langmuir–Blodgett techniques (two-dimensional)¹² or on a suitable substrate by controlled solvent evaporation (three-dimensional).¹⁰ Both approaches, however, are limited by the fact that only relatively simple nanocrystal architectures can be realized. For this reason, approaches that permit the assembly of complex nanocrystal architectures are of particular interest.

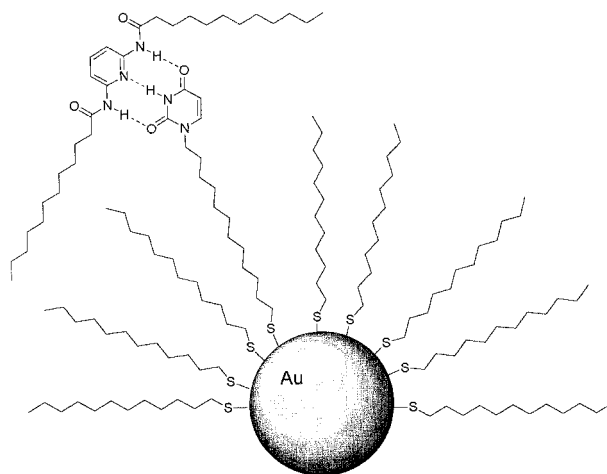
One possible approach is to adsorb stabilizer molecules incorporating a receptor site at the surface of a nanocrystal. It is expected that this nanocrystal will recognize and selectively bind another at which is adsorbed stabilizer molecules incorporating a complementary substrate site. By this means, the assembly of complex nanocrystal architectures in solution can be programmed.¹⁵

To date, TiO₂ nanocrystals stabilized by physisorbed long-chain alkanes incorporating a receptor site (uracil moiety) have been programmed to recognize and selectively bind in solution TiO₂ nanocrystals stabilized by physisorbed long-chain alkanes incorporating a substrate site (diaminopyridine moiety).¹⁶ Limited ordering of the constituent nanocrystals was apparent in the mesoaggregates formed as a result.

While encouraging, the specific approach outlined above has a number of limitations. Among these are the following. First, the stabilizer molecules, incorporating either a receptor or substrate site, were not chemisorbed at the nanocrystal surface. Second, the modified nanocrystals were not size-monodisperse.

To address the first of these limitations, a methodology was developed that permits the controlled chemisorption of a stabilizer molecule, incorporating the desired receptor or

SCHEME 1



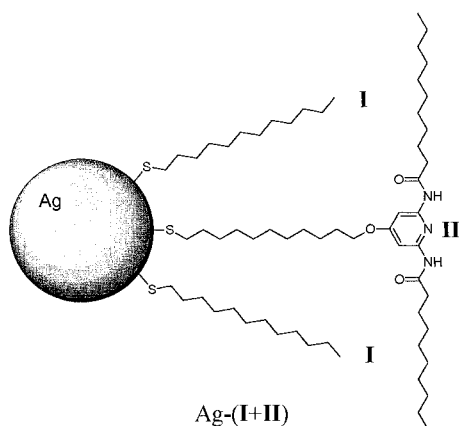
substrate site, at the surface of the nanocrystals of a stable dispersion.¹⁷ This methodology was used to prepare size-polydisperse gold nanocrystals stabilized by a chemisorbed mixture of a long-chain alkane thiol, dodecane thiol (95%), and a long-chain dodecane thiol incorporating a receptor site, 12-mercapto-dodecyl-1-uracil (5%). It was established that these nanocrystals recognize and selectively bind in solution a long-chain alkane incorporating a complementary substrate site, *N,N*-2,6-pyridinediylbis[undecamide] (Scheme 1).

To address the second of these limitations, size-monodisperse silver nanocrystals stabilized by a chemisorbed long-chain alkane thiol, dodecane thiol **I** (82%), and a chemisorbed long-chain alkane thiol incorporating a receptor site, *N,N*-2,6-pyridinediylbis[undecamide]-4-oxy-[12-mercapto dodecanyl] **II** (8%), have been prepared (Scheme 2). These nanocrystals and their dispersions are denoted Ag-(**I**+**II**). Size-monodisperse silver nanocrystals, stabilized by a chemisorbed long-chain alkane thiol incorporating a receptor site, **II** (100%), have also been prepared. These nanocrystals and their dispersions are denoted Ag-**II**.

When dispersed in chloroform, it was expected that Ag-(**I**+**II**) and Ag-**II** would recognize and selectively bind long-chain alkanes incorporating two complementary substrate sites, (1,12-

* Corresponding author.

SCHEME 2



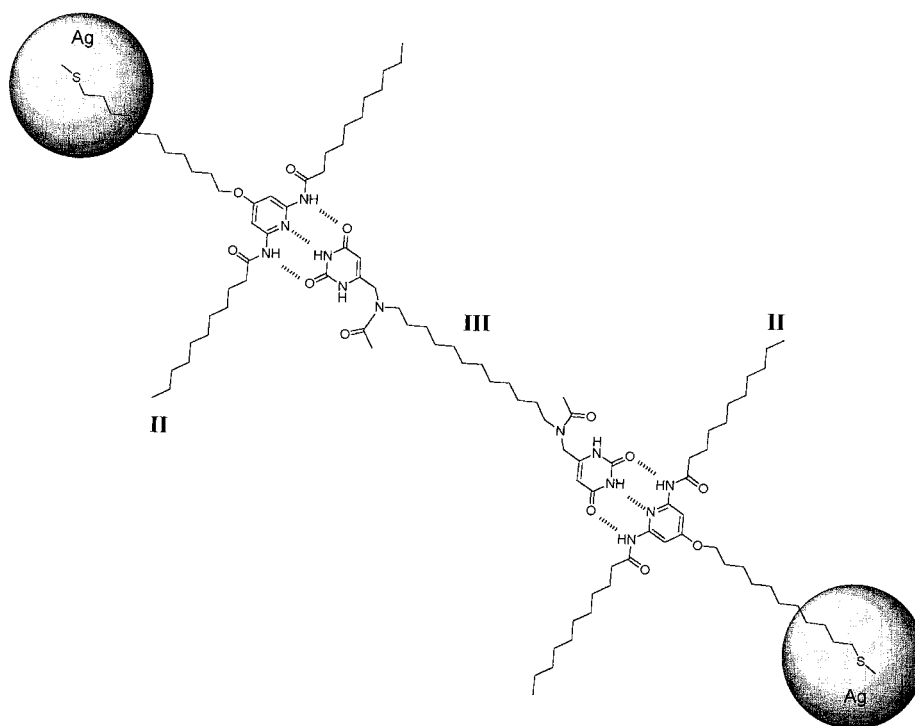
acetoamide dodecane) bis-6-methyluracil **III** (Scheme 3). It was also expected that the ability of **III** to be bound by two receptor sites on different nanocrystals would promote aggregation of Ag-(I+II) and Ag-II. NMR, FT-IR, and dynamic light scattering (DLS) have all been used to study the kinetics of aggregation of these nanocrystals and the structure of the aggregates formed.

The principal objectives of this study were the following. First, characterize the interactions at the molecular level between the receptor modified nanocrystals and the bifunctional substrates in solution that lead to nanocrystal aggregation. Second, to gain insights into the factors that control the size, shape and structure of the nanocrystal aggregates formed as a result.

Experimental Section

Synthesis of Stabilizer-Receptor and Substrate Molecules. Compound **I** was used as supplied by Aldrich. Compound **II** was prepared as shown (Scheme 4). Compound **III** was prepared as shown (Scheme 5). Compound **IV** was prepared as described in detail elsewhere.¹⁵ All molecules were characterized by elemental analysis and ¹H NMR.

SCHEME 3



Anal. Calcd. for **I** (C₁₂H₂₆S): C, 71.21; H, 12.95; S, 15.89. Found: C, 71.19; H, 13.12; S, 15.55. ¹H NMR (chloroform-*d*): δ 0.88 (t, 3H, *J* = 7.0 Hz); δ 1.26 (s, 18H); δ 1.61 (q, 2H, *J* = 7.3 Hz); δ 2.52 (q, 2H, *J* = 7.0 Hz).

Anal. Calcd. for **II** (C₄₁H₇₅N₃O₃S): C, 71.48; H, 10.74; N, 6.10; S, 4.65. Found: C, 70.75; H, 10.63; N, 5.59; S, 4.35. ¹H NMR (chloroform-*d*): δ 0.89 (t, 6H, *J* = 6.8 Hz); δ 1.28–1.44 (m, 48H); δ 1.68–1.79 (m, 8H); δ 2.36–2.39 (t, 4H, *J* = 7.3 Hz); δ 2.69–2.72 (t, 2H, *J* = 7.3 Hz); δ 4.03–4.06 (t, 2H, *J* = 6.3 Hz); δ 7.56 (s, 2H); δ 7.64 (s, 2H).

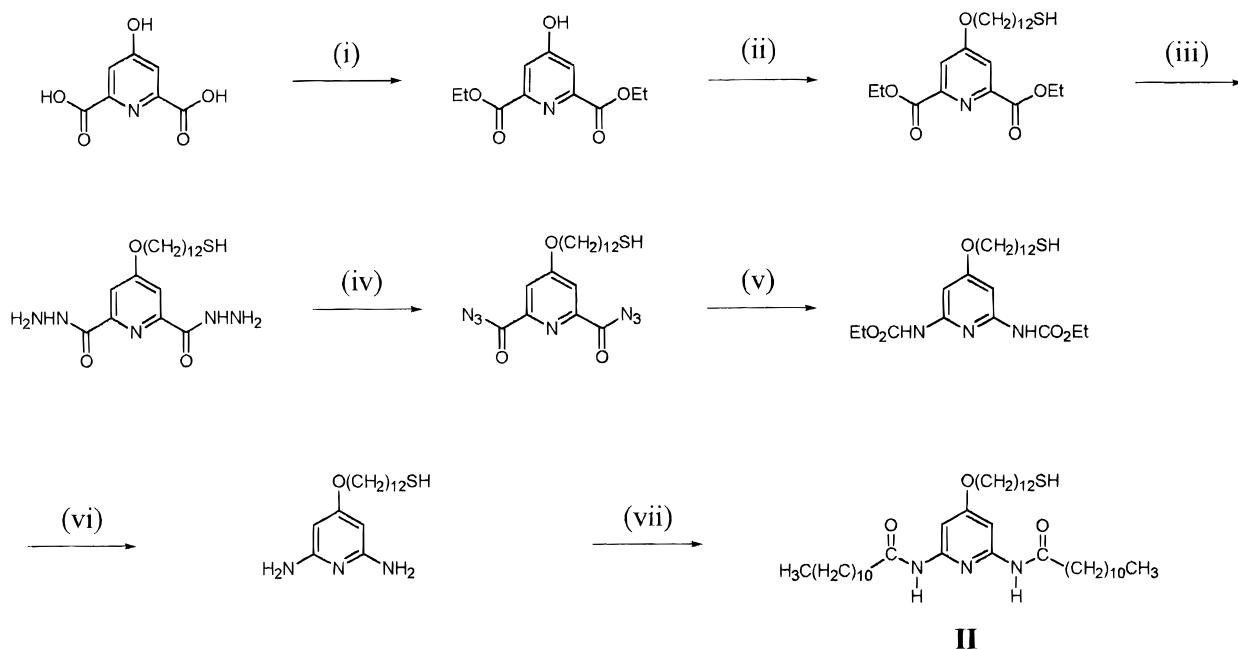
Anal. Calcd. for **III** (C₂₆H₄₀N₆O₆): C, 58.66; H, 7.51; N, 15.78. Found: C, 53.92; H, 6.90; N, 13.87. ¹H NMR (chloroform-*d*): δ 1.26–1.64 (m, 20H); δ 2.22 (s, 6H); δ 3.35–3.41 (t, 4H, *J* = 7.31 Hz); δ 4.26 (s, 4H); δ 5.60 (s, 2H); δ 9.50 (s, 2H); δ 9.70 (s, 2H).

Anal. Calcd. for **IV** (C₂₈H₅₁N₃O₃): C, 70.44; H, 10.69; N, 8.80. Found: C, 71.25; H, 10.95; N, 8.95. ¹H NMR (chloroform-*d*): δ 0.88 (t, 6H, *J* = 7.0 Hz); δ 1.26–1.58 (m, 40H); δ 2.36 (t, 2H, *J* = 7.8 Hz); δ 4.16 (s, 2H); δ 5.52 (s, 1H); δ 8.14 (s, 1H, –NH amidic); δ 9.51 (s, 1H, –NH imidic).

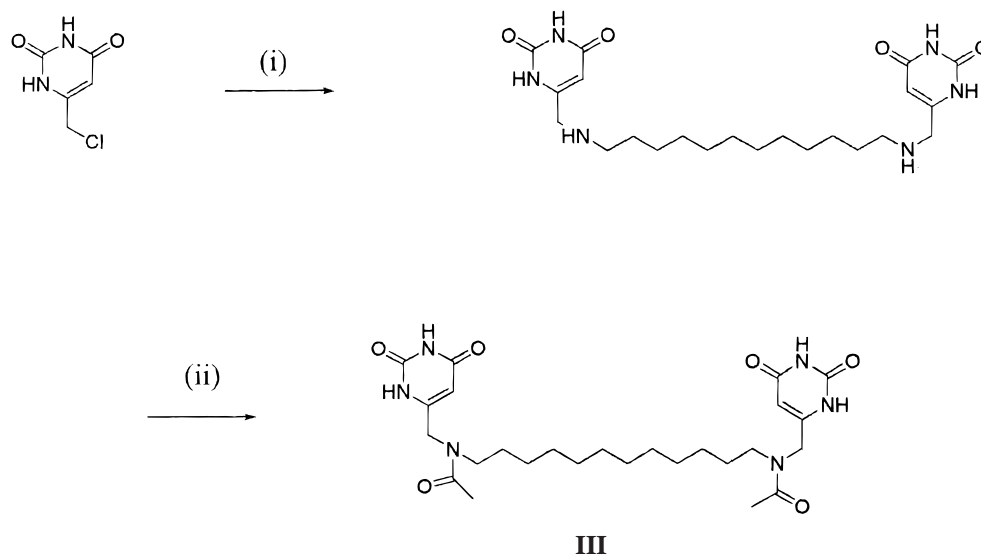
Preparation of Receptor-Modified Nanocrystals. Ag-I and Ag-(I+II) were prepared following the method of Brust et al.¹⁸ Briefly, AgNO₃ (0.154 g) was dissolved in H₂O (30 mL) and the phase transfer catalyst (C₈H₁₇)₄NBr (2.228 g), dissolved in chloroform (30 mL) and added with stirring for 1 h. A solution of **I** (0.825 g) or a mixed solution (80:20 mole ratio) of **I** (0.066 g) and **II** (0.057 g) in chloroform (8 mL) was then added (Ag/S mole ratio of approximately 1:1). After stirring for 2 to 3 min, the reducing agent NaBH₄ (0.394 g), dissolved in H₂O (24 mL), was added and stirring continued overnight. The nanocrystals formed were precipitated, filtered, and washed (using ethanol) to obtain a dry gray powder redispersible in chloroform.

Ag-II was prepared using a related approach. Briefly, AgNO₃ (0.154 g) was dissolved in H₂O (30 mL) and the phase transfer catalyst, (C₈H₁₇O₄)NBr (2.228 g) dissolved in chloroform (30 mL), was added with stirring for 1 h. At this point the silver salt was reduced by addition of NaBH₄ (0.394 g) in H₂O (24

SCHEME 4: Reagents and Conditions: (i) EtOH, 2% H₂SO₄, Reflux, (12 h); (ii) K₂CO₃, Br(CH₂)₁₂SH, Acetone (dry), Reflux (72 h); (iii) EtOH, N₂H₄, Reflux (3 h); (iv) 2M HCl, NaNO₂, H₂O; (v) EtOH, Reflux (24 h); (vi) Ethanolic KOH, Reflux (4 h); (vii) Pyridine (dry), Lauryl Chloride, CHCl₃ (dry)



SCHEME 5: Reagents and Conditions: (i) H₂N(CH₂)₁₂NH₂, CH₃CN, Reflux, (12 h); (ii) Acetyl Chloride, CHCl₃ (dry), Pyridine (dry)



mL). The chloroform phase was concentrated prior to precipitation of the silver nanocrystals by addition of a large volume of ethanol and their recovery by centrifugation. The phase transfer catalyst stabilized silver nanocrystals (20 mg) were redispersed in acetone (4 mL) to which **II** (40 mg) in chloroform (4 mL) was added. After stirring for 6 days, these nanocrystals were precipitated by addition of a large volume of ethanol. The precipitated nanocrystals were filtered and washed with ethanol to obtain a dry gray powder redispersible in chloroform.

Characterization Techniques. ¹H NMR spectra were obtained using either a JEOL JNM-GX270 FT or Varian 500 FT spectrometer. FT-IR spectra were obtained using a Mattson Infinity FT spectrometer and a CaF₂ cell (0.20 mm path length).

Dynamic light scattering (DLS) studies were performed using a Malvern PCS-4700 instrument equipped with a 256 channel correlator. The 488.0 nm line of a Coherent Innova-70 Ar ion

laser was used as the light source (100 mW). The temperature was maintained at 25 °C ± 0.02 °C throughout by an external circulator. All samples were filtered through 0.02 μm inorganic Anotop filters. Having been established that effects due to absorption at 488.0 nm by the silver nanocrystals are negligible, a silver nanocrystal concentration of 9.0 × 10⁻¹⁰ mol dm⁻³ was used. Additions to nanocrystal dispersions were made using a calibrated microsyringe and solutions previously filtered through 0.02 μm inorganic Anotop filters.

Transmission electron micrographs (TEMs) were obtained using a JEOL TEMSCAN 2000 EX and graphite coated copper grids.

Results and Discussion

Characterization of Receptor-Modified Nanocrystals. Silver nanocrystals stabilized by the alkane thiol **I** and the modified

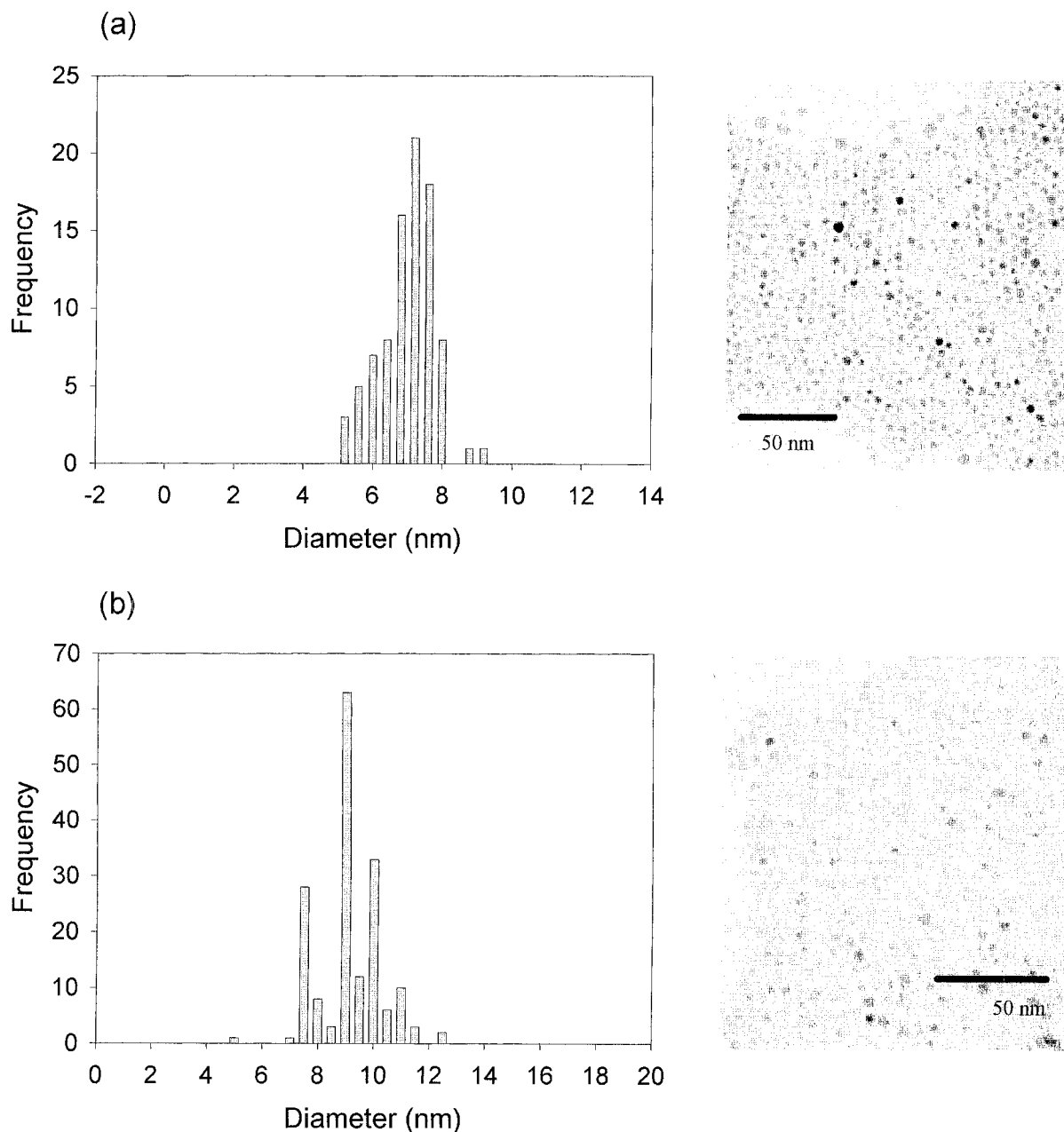


Figure 1. (a) TEM of Ag-(I+II) and histogram nanocrystal diameters determined from image. (b) As in (a) for Ag-II.

alkane thiol incorporating a receptor site **II**, Ag-(I+II), have been characterized by TEM and elemental analysis as described in detail elsewhere.^{17–19} It has been established by TEM that these nanocrystals have a spherical silver core that is 71 Å in diameter, a size polydispersity of less than 10% and, as can be seen from Figure 1, form a hexagonally close-packed array upon solvent evaporation.²⁰ It has been further established by elemental analysis that there are on average 957 molecules adsorbed at the surface of each nanocrystal and that the ratio of I:II is 12:1.²¹ On this basis, and assuming that the average area occupied by a molecule of **II** adsorbed at the surface of a silver nanocrystal is 23 Å² (see below), it is calculated that the average area occupied by a molecule of **I** adsorbed at the surface of a silver nanocrystal is 16 Å². This value agrees well with those previously reported for alkane thiols adsorbed at the surface of a silver nanocrystal.^{17,19}

Silver nanocrystals stabilized by adsorbed alkane thiol incorporating a diaminopyridine receptor site **II**, Ag-II, have also been characterized by TEM and elemental analysis. It has

been established by TEM that these nanocrystals have a spherical silver core that is 88 Å in diameter, a size polydispersity of less than 5% and, as can be seen from Figure 1, form a hexagonally close-packed array upon solvent evaporation.²² It has been established by elemental analysis that there are on average 1088 molecules of **II** adsorbed at the surface of each nanocrystal.²³ On this basis it is calculated that the average area occupied by the stabilizer molecules adsorbed at the surface of a silver nanocrystal is 23 Å², the value assumed above. This value, as might have been expected, is somewhat larger than values previously reported for unmodified alkane thiols adsorbed at the surface of a silver nanocrystal.^{17,19}

Receptor-Substrate Binding in Solution. To establish that the diaminopyridine receptor site incorporated in **II** recognizes and selectively binds the complementary uracil substrate sites incorporated in **III** to form a 2:1 complex, the ¹H NMR and FT-IR spectra of **II**, **III**, and different mixtures of **II** and **III** were measured in chloroform-*d* at 25 °C.

Shown in Figure 2 are the ¹H NMR spectra of **II** (1.45 ×

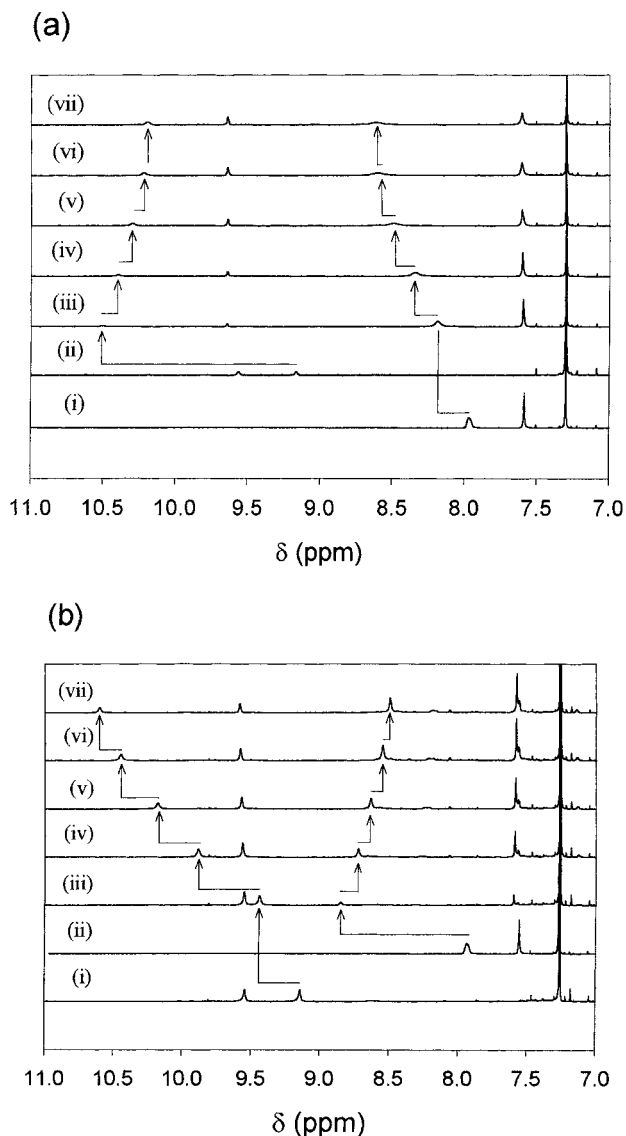


Figure 2. (a) ^1H NMR spectra of (i) **II** ($1.45 \times 10^{-3} \text{ mol dm}^{-3}$) and (ii) **III** ($0.36 \times 10^{-3} \text{ mol dm}^{-3}$) in chloroform-*d* at 25 °C. Also shown are the ^1H NMR spectra of **II** ($1.45 \times 10^{-3} \text{ mol dm}^{-3}$) in chloroform at 25 °C to which the following molar equivalents of **III** ($0.36 \times 10^{-3} \text{ mol dm}^{-3}$) have been added: (iii) 0.25; (iv) 0.50; (v) 0.75; (vi) 1.00; and (vii) 1.25. (b) ^1H NMR spectra of (i) **III** ($1.88 \times 10^{-3} \text{ mol dm}^{-3}$) and (ii) **II** ($0.47 \times 10^{-3} \text{ mol dm}^{-3}$) in chloroform-*d* at 25 °C. Also shown are the ^1H NMR spectra of **III** ($1.88 \times 10^{-3} \text{ mol dm}^{-3}$) in chloroform at 25 °C to which the following molar equivalents of **II** ($0.47 \times 10^{-3} \text{ mol dm}^{-3}$) have been added: (iii) 0.25; (iv) 0.50; (v) 0.75; (vi) 1.00; and (vii) 1.25.

$10^{-3} \text{ mol dm}^{-3}$) prior to and following addition of the indicated number of molar equivalents of **III** (relative to **II**) in 0.25 molar equivalent amounts. Also shown is the spectrum of **III** ($0.36 \times 10^{-3} \text{ mol dm}^{-3}$, 0.25 molar equivalent).

The resonance assigned to the amidic protons of **II** is observed at δ 7.96, while the resonances assigned to the imidic and amidic protons of **III** are observed at δ 9.16 and δ 9.56, respectively. Following each addition of 0.25 of an equivalent of **III** to **II** there is a downfield shift in the amidic proton resonance of **II** by about δ 0.1. After 1.25 equivalents of **III** are added, the amidic proton resonance of **II** is shifted downfield to δ 8.61. Following addition of 0.25 of an equivalent of **III** to **II** there is a downfield shift in the imidic proton resonance of **III** to δ 10.50. Each subsequent addition of 0.25 of an equivalent of **III** is accompanied by a small upfield shift. After 1.25 equivalents

of **III** are added the imidic resonance of **III** is shifted upfield to 10.19. The resonance assigned amidic proton of **III** is observed at δ 9.56 throughout.

Also shown in Figure 2 are the ^1H NMR spectra of **III** ($1.88 \times 10^{-3} \text{ mol dm}^{-3}$) prior to and following addition of the indicated number of molar equivalents of **II** (relative to **III**) in 0.25 molar equivalent amounts. Also shown is the spectrum of **II** ($0.47 \times 10^{-3} \text{ mol dm}^{-3}$, 0.25 molar equivalent).

Following each addition of 0.25 of an equivalent of **II** to **III** there is a downfield shift in the imidic proton resonance of **III** by about δ 0.25. After 1.25 equivalents of **II** are added, the amidic proton resonance of **IV** is shifted downfield to δ 10.64. Following addition of 0.25 of an equivalent of **II** to **III** there is a downfield shift in the amidic proton resonance of **II** to δ 8.88. Each subsequent addition of 0.25 of an equivalent of **II** is accompanied by a small upfield shift. After 1.25 equivalents of **II** are added, the amidic resonance of **II** is shifted upfield to 8.53. The resonance assigned amidic proton of **III** is observed at δ 9.56 throughout.

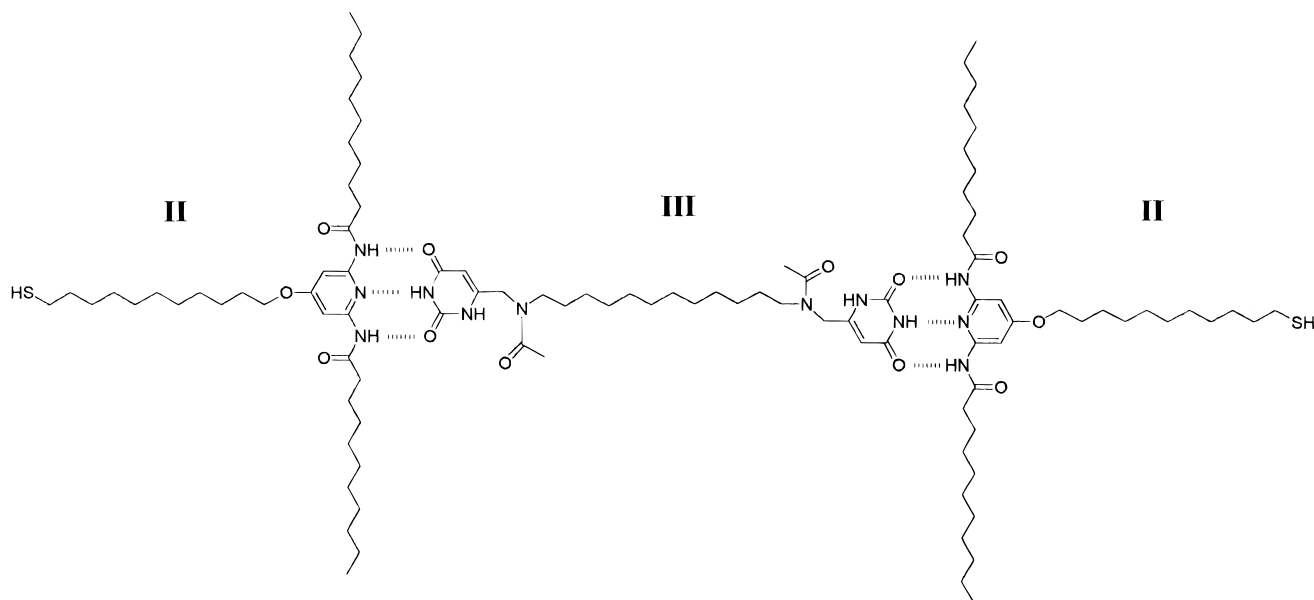
These findings are understood as follows. Upon addition of 0.25 of an equivalent of **III** to **II**, a large fraction both substrate sites of **III** is complexed to **II**, while only a small fraction of **II** is complexed to **III**. As a consequence, the resonance assigned to the imidic proton of **III** is shifted downfield to a value characteristic of **III** in the 2:1 complex shown in Scheme 6 and associated by two triple arrays of complementary hydrogen bonds.²⁴ Under the same conditions the resonance assigned to the amidic proton of **II** is shifted downfield, but only by a small amount, to a value that remains characteristic of **II** in solution.²⁴ In the course of four subsequent additions of 0.25 equivalents of **III**, the resonance assigned to the imidic proton of **III** is observed to shift back upfield as the fraction of uncomplexed **III** present in solution increases. Under the same conditions, the resonance assigned to the amidic proton in **II** is shifted downfield to a value characteristic of the complex shown in Scheme 6. Analogous observations made upon addition of **II** to **III** are consistent with formation the 2:1 complex shown in Scheme 6 and are associated by two triple arrays of complementary hydrogen bonds.

It should be noted that because the dynamics of complex formation are fast on the NMR time scale, the chemical shifts observed for the amidic and imidic peak positions are the population-weighted average of chemical shifts of **II** and **III** in the complexed and uncomplexed states. For this reason the end point of a titration is not well defined. It should also be noted that the chemical shifts of the amidic and imidic resonances in **II** and **III** are concentration dependent.

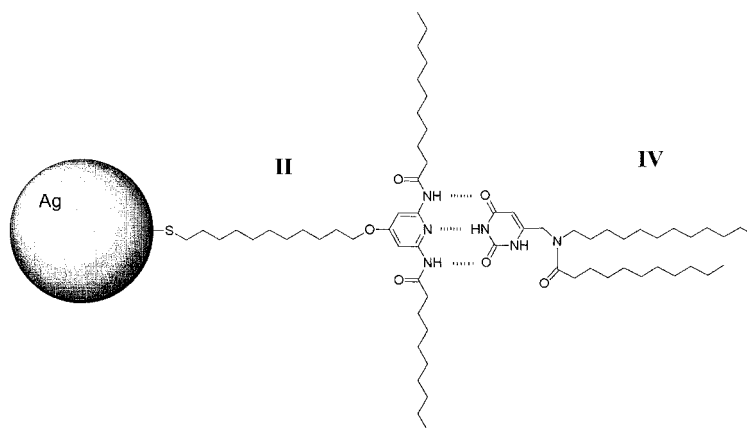
Shown in Figure 3 are the FT-IR spectra of **II** ($2.90 \times 10^{-3} \text{ mol dm}^{-3}$), **III** ($1.45 \times 10^{-3} \text{ mol dm}^{-3}$), and a mixture of **II** ($2.90 \times 10^{-3} \text{ mol dm}^{-3}$) and **III** ($1.45 \times 10^{-3} \text{ mol dm}^{-3}$) in chloroform-*d* at 25 °C. The bands at 3420 and 3392 cm^{-1} are assigned to the amidic N–H stretches of **II** and **III**, respectively.²⁵ On preparing the above mixture of **II** and **III**, the intensity of the bands assigned to the free amidic N–H stretches decreases.²⁶ Also on preparing the above mixture of **II** and **III**, a series of bands between 3200 and 3300 cm^{-1} , assigned to the hydrogen-bonded amidic protons are newly observed.²⁷ These findings are consistent with formation of a 2:1 complex between **II** and **III** associated by formation of two triple arrays of complementary hydrogen bonds,²⁸ and therefore are also consistent with the findings of the ^1H NMR studies reported above.

It is clear, based on the findings presented above, that a modified alkane thiol incorporating a diaminopyridine receptor

SCHEME 6



SCHEME 7



site recognizes and selectively binds a modified alkane thiol incorporating two uracil substrate sites. The question which

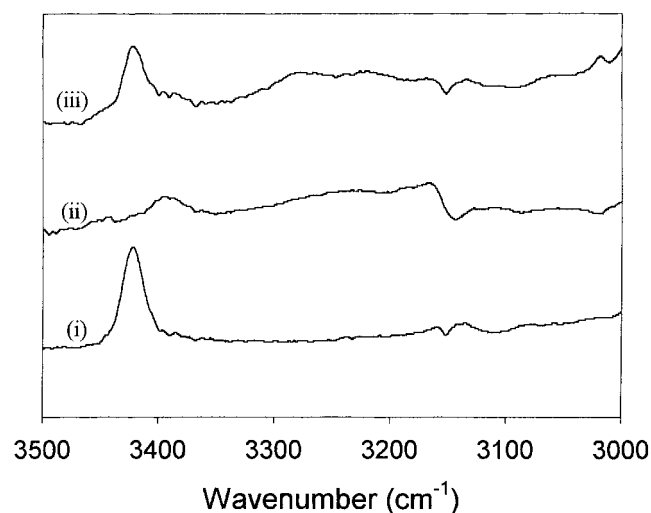


Figure 3. FTIR spectra of (i) **II** ($2.90 \times 10^{-3} \text{ mol dm}^{-3}$) and (ii) **III** ($1.45 \times 10^{-3} \text{ mol dm}^{-3}$) in chloroform-*d* at 25 °C. Also shown is the FTIR spectrum (iii) of a 2:1 molar ratio mixture of **II** ($2.90 \times 10^{-3} \text{ mol dm}^{-3}$) and **III** ($1.45 \times 10^{-3} \text{ mol dm}^{-3}$) in chloroform at 25 °C.

arises next is whether silver nanocrystals stabilized by an alkane thiol incorporating a diaminopyridine receptor site will also recognize and selectively bind a modified alkane thiol incorporating two uracil substrate sites.

Receptor-Modified Nanocrystal–Substrate Binding in Solution. Presented are the findings of ^1H NMR and FTIR studies which establish that silver nanocrystals stabilized by **II**, specifically Ag-(**I+II**), recognize and selectively bind **IV** in solution. That is, findings which establish that the diaminopyridine receptor site incorporated in **II** continues to recognize and selectively bind the complementary uracil substrate site incorporated in **IV**, even when chemisorbed at the surface of a silver nanocrystal (Scheme 7).

Shown in Figure 4 are the ^1H NMR spectra of Ag-(**I+II**) ($1.88 \times 10^{-5} \text{ mol dm}^{-3}$ silver nanocrystals, $1.40 \times 10^{-3} \text{ mol dm}^{-3}$ **II**) in chloroform-*d* at 25 °C prior to and following successive additions of 0.15 molar equivalents of **IV** (with respect to **II**). Also shown is the spectrum of **IV** ($0.21 \times 10^{-3} \text{ mol dm}^{-3}$, 0.15 molar equivalents) in chloroform-*d* at 25 °C.

Initially, the resonances assigned to the amidic protons of **II** in Ag-(**I+II**) are observed at δ 7.55, while the resonances assigned to the imidic and amidic protons of **IV** are observed at δ 7.65 and δ 9.35, respectively. Following addition of 0.15 molar equivalents of **IV** to the Ag-(**I+II**) dispersion, the amidic

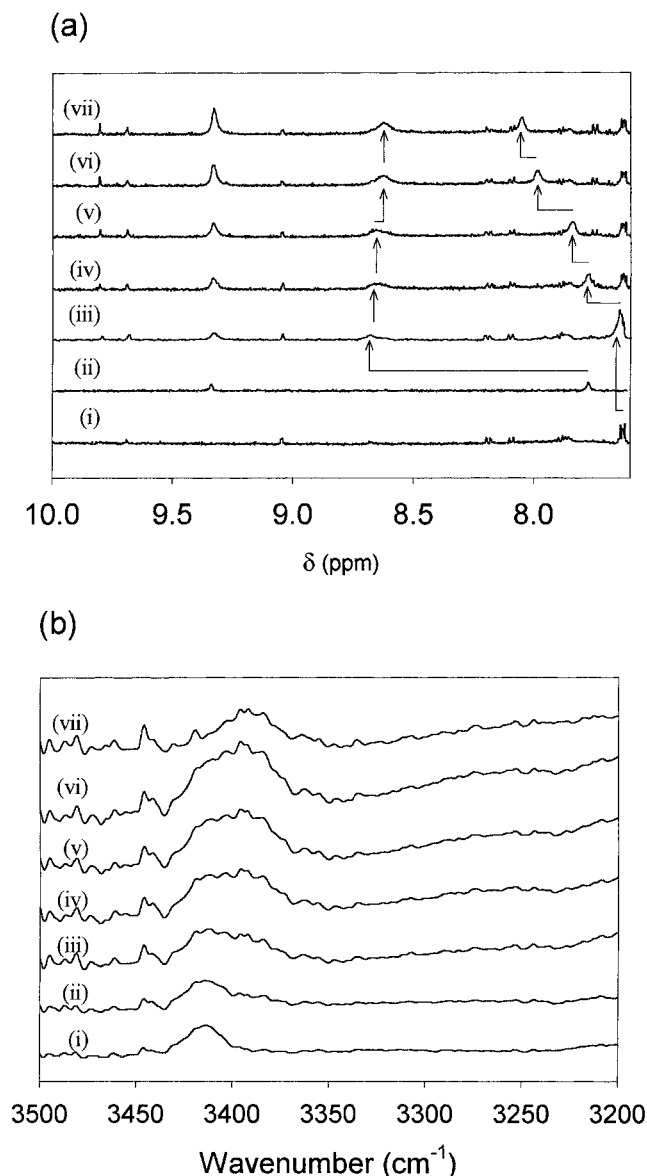


Figure 4. (a) ¹H NMR spectra of (i) Ag-(**I+II**) (1.88×10^{-5} mol dm⁻³ nanocrystals, 1.40×10^{-3} mol dm⁻³ **II**) and (ii) **IV** (0.21×10^{-3} mol dm⁻³) in chloroform-*d* at 25 °C. Also shown are the ¹H NMR spectra of Ag-**II** (1.88×10^{-5} mol dm⁻³ nanocrystals, 1.40×10^{-3} mol dm⁻³ **II**) in chloroform at 25 °C to which the following molar equivalents of **IV** (0.21×10^{-3} mol dm⁻³) have been added: (iii) 0.15; (iv) 0.30; (v) 0.45; (vi) 0.60; and (vii) 0.75. (b) FTIR spectra measured under same conditions as in (a).

proton resonance of **II** is shifted downfield to δ 7.65. After addition of a total of 0.75 molar equivalents of **IV**, this resonance is shifted downfield to δ 8.07. Following addition of 0.15 of an equivalent of **IV** to Ag-(**I+II**), the resonance assigned to the imidic proton resonance of **IV** is shifted downfield to δ 8.69. Each subsequent addition of 0.15 of an equivalent of **IV** is accompanied by a small upfield shift. After 0.75 equivalents of **IV** are added this resonance is shifted upfield to δ 8.64. The resonance assigned amidic proton of **IV** is observed at δ 9.35 throughout, implying that it is not involved in complexation.

Also shown in Figure 4 are the FTIR spectra of Ag-(**I+II**) (1.88×10^{-5} mol dm⁻³ silver nanocrystals, 1.40×10^{-3} mol dm⁻³ **II**) in chloroform-*d* at 25 °C prior to and following successive additions of 0.15 molar equivalents of **IV** (with respect to **II**). Also shown is the spectrum of **IV** (0.21×10^{-3} mol dm⁻³, 0.15 molar equivalent) in chloroform-*d* at 25 °C.

The band at 3420 cm⁻¹ is assigned to the amidic stretches of **II**. The band at 3392 cm⁻¹ is assigned to the imidic N–H stretch of **IV**. It is observed that the intensity of the band assigned to the amidic N–H stretch of **II** decreases as the concentration of added **IV** increases. At the same time, the increase in intensity of the band assigned to the imidic N–H stretch of **IV** is less than that observed for the same concentration of **IV** in solution. The newly observed bands between 3300 cm⁻¹ and 3200 cm⁻¹ are assigned to formation of the hydrogen bonds between the receptor and substrate.

It is clear, based on the ¹H NMR and FT-IR findings presented above, that a silver nanocrystal stabilized by an alkane thiol and an alkane thiol incorporating a receptor site, namely Ag-(**I+II**), recognizes and selectively binds in solution a molecule incorporating a complementary substrate site, namely **IV**. Furthermore, it is also clear that the resulting 1:1 complex is noncovalently associated by a triple array of hydrogen bonds as shown in Scheme 7.

It should be noted that these detailed studies were not undertaken using the modified alkane thiol incorporating two uracil substrate states, namely **III**. The reason for this, as discussed in detail below, is that the addition of **III** to Ag-(**I+II**) promotes nanocrystal aggregation, thereby precluding detailed characterization of the molecular interactions leading to aggregation by NMR and to a lesser extent by FT-IR.

Aggregation of Receptor-Modified Nanocrystals in Solution. A question which arises is whether the ability to program a size-monodisperse silver nanocrystal to recognize and selectively bind a molecular substrate in solution can be exploited to assemble complex and technologically relevant nanocrystal assemblies, also in solution.

With respect to this question, we note that a large number of studies have been directed toward understanding the mechanisms of colloid aggregation and their relationship to the structure of the aggregates formed.²⁹ Generally, two limiting cases have been identified.^{30,31} The first, termed slow or reaction-limited aggregation, refers to the case where only a small fraction of the collisions result in the two colloidal particles involved adhering to each other.³⁰ It has been found that the growth kinetics of reaction-limited aggregation are described by eq 1

$$R_h(t) = R_h(t_0) \exp(ct) \quad (1)$$

where $R_h(t_0)$ is the initial hydrodynamic radius of the aggregate, typically determined by dynamic light scattering, and c is a parameter characteristic of the experimental conditions. Related static light scattering experiments have established that the fractal dimension of such aggregates is 2.05.

The second case, termed fast or diffusion-limited aggregation, refers to the situation where each collision results in the two colloidal particles involved adhering to each other.³¹ It has been found that the growth kinetics of diffusion-limited aggregation are described by eq 2

$$R_h(t) \propto t^{1/d_f} \quad (2)$$

where $R_h(t)$ is the hydrodynamic radius of the aggregate at some time t , determined by dynamic light scattering, and d_f is the fractal dimension which has a value of 1.75.

The associated physical picture can be summarized as follows. In the reaction-limited regime, the particles have a low probability of adhering upon contact, sample many possible configurations, and form aggregates which are relatively dense, possibly locally ordered, and have a fractal dimension of 2.05. In the diffusion-limited regime, the particles have a high

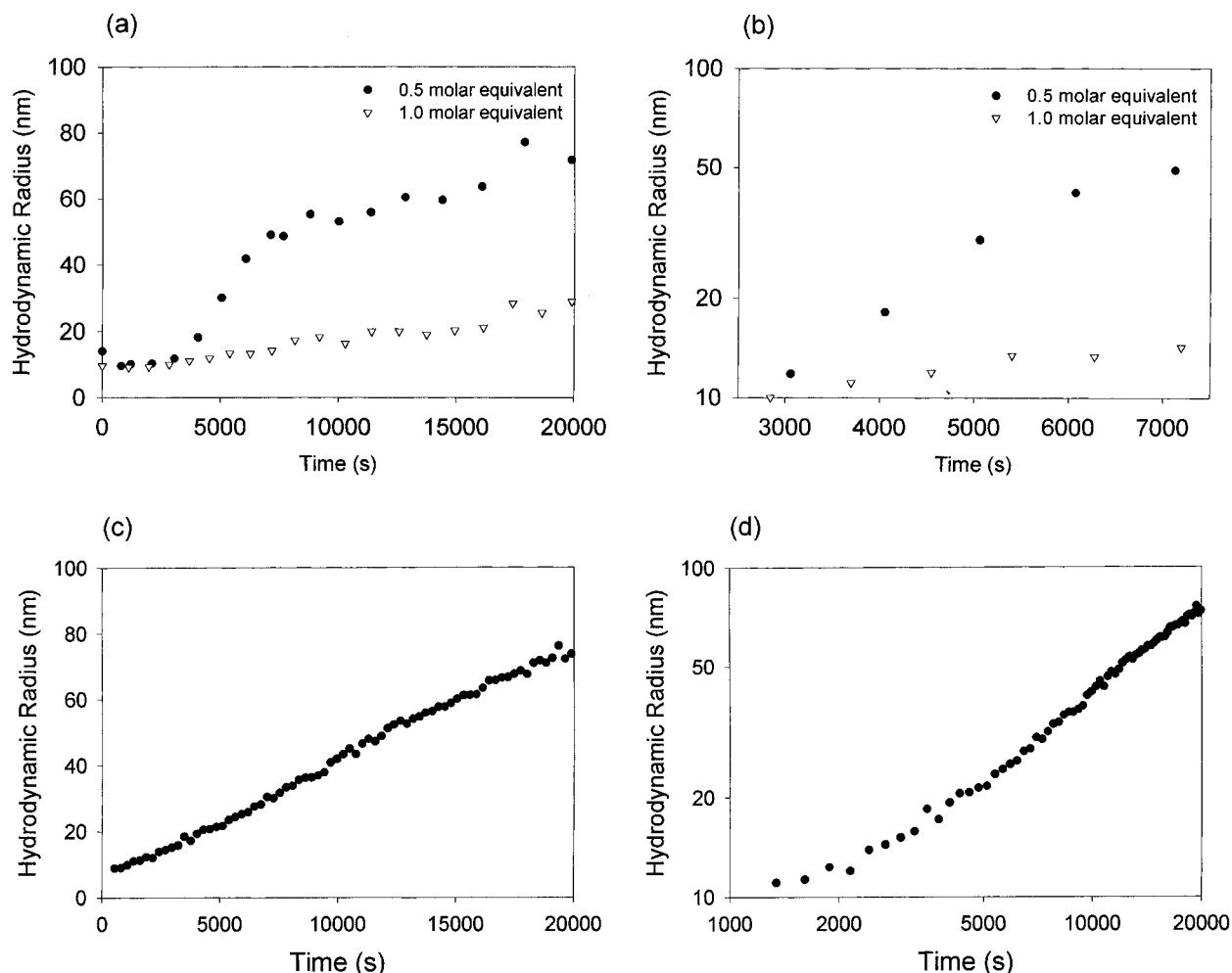


Figure 5. (a) Hydrodynamic radius of Ag-(**I+II**) ($3.29 \times 10^{-8} \text{ mol dm}^{-3}$ nanocrystals, $2.43 \times 10^{-6} \text{ mol dm}^{-3}$ **II**) plotted against elapsed time in chloroform at 25 °C to which has been added 0.5 ($1.21 \times 10^{-6} \text{ mol dm}^{-3}$) and 1.0 ($2.43 \times 10^{-6} \text{ mol dm}^{-3}$) molar equivalents of **III**. (b) Semilog plot of data in (a). (c) Hydrodynamic radius of Ag-(**I+II**) ($3.29 \times 10^{-8} \text{ mol dm}^{-3}$ nanocrystals, $3.58 \times 10^{-5} \text{ mol dm}^{-3}$ **II**) plotted against elapsed time in chloroform at 25 °C to which has been added 0.5 ($1.79 \times 10^{-5} \text{ mol dm}^{-3}$) molar equivalents of **III**. (d) Log-log plot of data in (c).

probability of adhering upon contact, sample few possible configurations, and form relatively diffuse aggregates, probably locally branch-like, and which have fractal dimension of 1.75.

The above summary description of particle aggregation assumes that nanocrystal motion is diffusive and that particle-particle aggregation is homogeneous. Furthermore, it assumes that particle aggregation is irreversible with little subsequent reorganization of the aggregate structure. In practice, there are cases in which two particles have a high probability of adhering upon contact and in which the kinetics of aggregate growth are diffusion limited, but in which the strength of the interaction between aggregated particles is sufficiently small that significant restructuring leads to a larger fractal dimension.³²

The previous sections of this paper have described the preparation and characterization of size-monodisperse nanocrystals stabilized by chemisorption of alkane thiols and alkane thiols incorporating a receptor site (diaminopyridine), namely Ag-(**I+II**) or Ag-**II**. The present paper has also established that these receptor modified nanocrystals recognize and selectively bind molecules incorporating a substrate site (uracil), namely **IV**. As a consequence, it should prove possible to induce aggregation of either Ag-(**I+II**) or Ag-**II** by addition of 0.5 molar equivalents (with respect to **II**) of **III**, corresponding to 1.0 molar equivalent of substrate sites, to these dispersions. It was expected that, in the case of Ag-(**I+II**), with an 8%

coverage of receptor sites, aggregation would be reaction-limited, but that in the case of Ag-**II**, with a 100% coverage of receptor sites, that aggregation would be diffusion-limited. To test these expectations the aggregation kinetics of Ag-(**I+II**) and Ag-**II** dispersions containing added **III** have been studied by DLS.

Shown in Figure 5 are the hydrodynamic radii measured by DLS in chloroform-*d* at 25 °C for two Ag-(**I+II**) dispersions ($3.29 \times 10^{-8} \text{ mol dm}^{-3}$ concentration of silver nanocrystals, $2.43 \times 10^{-6} \text{ mol dm}^{-3}$ concentration of adsorbed receptor sites in **II**) to which have been added 0.50 ($1.21 \times 10^{-6} \text{ mol dm}^{-3}$) or 1.00 ($2.42 \times 10^{-6} \text{ mol dm}^{-3}$) molar equivalents of **III** with respect to **II**. As there are two substrate sites incorporated in **III**, this corresponds to 1.00 and 2.00 substrate site equivalents, respectively.

Having added 0.50 of a molar equivalent of **III** with respect to **II**, or 1.00 substrate equivalents with respect to the receptor, to a dispersion of Ag-(**I+II**) it was expected that a fraction of **III**, containing two substrate sites, would bind receptor sites on different Ag-(**I+II**) nanocrystals and that this would lead to nanocrystal aggregation. This expectation is seen to be well founded as the average hydrodynamic radius increased by more than 60 nm during 2 h.

Having added 1.00 molar equivalent of **III** with respect to **II**, or 2.00 substrate equivalents with respect to the receptor, to

a dispersion of Ag-(I+II), it was expected that each molecule of III, containing two substrate sites, would in the majority of cases bind only a single receptor site on a Ag-(I+II) nanocrystal and that this would inhibit nanocrystal aggregation. This expectation is also seen to be well founded as the average hydrodynamic radius increased by less than 10 nm during 2 h.

It is clear that the kinetics of aggregation of Ag-(I+II) induced by addition of 0.5 molar equivalents of III are slow and described by an expression of the general formula given in eq 1. Specifically, a semilog plot of the data in Figure 5a yields a straight line, see Figure 5b. On this basis it is concluded that aggregation is reaction-limited.^{29,30} This finding is consistent with a low probability of two receptor-modified silver nanocrystals aggregating upon collision and suggests that the nanocrystal aggregate formed most likely has a compact and relatively ordered structure. It is equally clear that the kinetics of aggregation of Ag-(I+II) induced by addition of 1.0 molar equivalents of III are still slower. On this basis it is concluded that aggregation is largely inhibited. This finding is consistent with all of the receptor sites being occupied by a molecule of III, as a consequence of which and as expected, aggregation is inhibited.

Also shown in Figure 5 are the hydrodynamic radii measured by DLS in chloroform-*d* at 25 °C for an Ag-II dispersion (3.29×10^{-8} mol dm⁻³ concentration of silver nanocrystals, 3.58×10^{-5} mol dm⁻³ concentration of adsorbed receptor sites in II) to which have been added 0.50 (1.79×10^{-5} mol dm⁻³) molar equivalents of III with respect to II. As there are two substrate sites incorporated in III, this corresponds to 1.00 of an equivalent of receptor sites.

Having added 0.50 molar equivalents of III with respect to II, or 1.00 substrate equivalents with respect to the receptor, to a dispersion of Ag-II, it was expected that the each molecule of III, containing two substrate sites, would bind receptor sites on different Ag-II nanocrystals and that this would lead to nanocrystal aggregation. This expectation is seen to be well founded as the average hydrodynamic radius, measured by dynamic light scattering, increased to 100 nm during 2 h.

It is clear that the kinetics of aggregation of Ag-II induced by addition of 0.5 molar equivalents of III are fast and described by an expression of the general formula given in eq 1. Specifically, a log-log plot of the data in Figure 5c yields a straight line of slope 0.68, see Figure 5d. On this basis it is concluded that aggregation is diffusion limited.^{29,31} This finding is consistent with a high probability of two receptor-modified silver nanocrystals aggregating upon collision and suggests that the nanocrystal aggregate formed most likely has an open and disordered structure.

It is noted that the reciprocal of the slope of the log-log plot referred to above yields a value for the fractal dimension of the aggregate formed.³¹ The value obtained (1.45) is significantly less than that expected (1.75). This finding is consistent with an earlier study of the salt-induced aggregation of polystyrene particles.³² This study reported that accurate values for the fractal dimension of the aggregate were obtained only from variable-angle static light scattering studies. The possibility that the initially formed aggregates were restructuring was considered.

Conclusions

Silver nanocrystals stabilized by a chemisorbed long-chain alkane thiol and a chemisorbed long-chain alkane thiol incorporating a diaminopyridine receptor site, Ag-(I+II), have been prepared. Silver nanocrystals stabilized only by a chemisorbed

long-chain alkane thiol incorporating a diaminopyridine receptor site, Ag-II, have also been prepared. When dispersed in chloroform these "programmed" nanocrystals recognize and selectively bind a long-chain alkane incorporating two complementary substrate sites, III, and are noncovalently linked. The nanocrystal aggregates formed as a result have been characterized by NMR, FT-IR, and DLS.

The key findings are that aggregation of Ag-(I+II) in the presence of added III is reaction limited, while aggregation of Ag-II in the presence of added III exhibits diffusion-limited kinetics. These findings demonstrate, for the first time, that the number of receptor sites present on the surface of a dispersion of nanocrystal can be used to control their aggregation kinetics. Angle-dependent static light scattering studies are in progress to better understand the relationship aggregation kinetics and the structures of the nanocrystal aggregates formed.

An implication of these findings is that to achieve the desired level of control over the architecture of structures assembled from nanocrystals in solution it will be necessary to be able to do the following: first, determine which nanocrystals recognize and selectively bind to each other and, second, determine the strength of the forces acting between nanocrystals. These forces should be such that reaction limited aggregation is followed by restructuring to yield a nanocrystal aggregate with the desired architectural properties.

A general insight based on the findings reported here is that the surface modification can be used to determine the aggregation kinetics and, as a consequence, the structure of aggregates formed by colloidal particles. It is expected that this insight will inform the work of scientists and technologists in diverse fields, ranging from medical diagnostics to electronics.

Acknowledgment. The authors thank the Petroleum Research Fund of the American Chemical Society for funding the reported study (ACS-PRF# 32897-ACS).

References and Notes

- (1) Alivisatos, A. P. *Science* **1996**, *271*, 933 and references therein.
- (2) Murray, C. B.; Norris, D. J.; Bawendi, M. G. *J. Am. Chem. Soc.* **1993**, *115*, 8706.
- (3) Andres, R. P.; Bielefeld, J. D.; Henderson, J. I.; Janes, D. B.; Kolagunta, V. R.; Kubiak, C. P.; Mahoney, W. J.; Osifchin, R. G. *Science* **1996**, *273*, 1690.
- (4) Vossmeier, T.; Katsikas, L.; Giersig, M.; Popovic, I. G.; Diesner, K.; Chemseddine, A.; Eychmueller, A.; Weller, H. *J. Phys. Chem.* **1994**, *98*, 7665.
- (5) Harfenist, S. A.; Wang, Z. L.; Alvarez, M. A.; Vezmar, I.; Whetten, R. L. *J. Phys. Chem.* **1996**, *100*, 13904.
- (6) Herron, N.; Calabrese, J. C.; Farneth, W. E.; Wang, Y. *Science* **1993**, *259*, 1426.
- (7) Schmidt, G. *Chem. Rev.* **1992**, *92*, 1709.
- (8) Moritz, T.; Reiss, K.; Diesner, K.; Su, D.; Chemseddine, J. *J. Phys. Chem. B* **1997**, *101*, 8052.
- (9) Brus, L. *J. Phys. Chem.* **1986**, *90*, 2555.
- (10) Murray, C. B.; Kagan, C. R.; Bawendi, M. G. *Science* **1995**, *270*, 1335.
- (11) Kagan, C. R.; Murray, C. B.; Bawendi, M. G. *Phys. Rev. B* **1996**, *54*, 8633.
- (12) Heath, J. R.; Knobler, C. M.; Leff, D. V. *J. Phys. Chem. B* **1997**, *101*, 189.
- (13) Motte, L.; Billoudet, F.; Lacaze, E.; Douin, J.; Pileni, M. P. *J. Phys. Chem. B* **1997**, *101*, 138.
- (14) Elghanain, R.; Storhoff, J.; Micic, R.; Letsinger, R.; Mirkin, C. *Science* **1997**, *277*, 1078.
- (15) (a) Cusack, L.; Rao, S. N.; Wenger, J.; Fitzmaurice, D. *Chem. Mater.* **1997**, *9*, 624. (b) Cusack, L.; Rao, S. N.; Fitzmaurice, D. *Chem. Eur. J.* **1997**, *3*, 202. (c) Cusack, L.; Marguerettaz, X.; Rao, S. N.; Wenger, J.; Fitzmaurice, D. *Chem. Mater.* **1997**, *9*, 1765.
- (16) Cusack, L.; Rizza, R.; Gorelov, A.; Fitzmaurice, D. *Angew. Chem., Int. Ed. Engl.* **1997**, *36*, 848.
- (17) Ahern, D.; Rao, S. N.; Fitzmaurice, D. *J. Phys. Chem. B* **1999**, *103*, 1821.

(18) Brust, M.; Walker, M.; Bethell, D.; Schiffrin, D.; Whyman, R. *J. Chem. Soc., Chem. Commun.* **1994**, 801.

(19) Korgel, B.; Fullam, S.; Connolly, S.; Fitzmaurice, D. *J. Phys. Chem.* **1998**, *102*, 8379.

(20) To obtain these values, the diameter of 300 silver nanocrystals modified by chemisorbed **I** and **II** were determined from a TEM image prepared by evaporation of a chloroformic dispersion of these nanocrystals on a carbon-coated copper grid. It is noted that these nanocrystals show long range ordering, an observation that strongly supports the assertion that these nanocrystals are relatively monodisperse.

(21) To obtain these values, a known weight of a sample silver nanocrystals modified by chemisorbed **I** and **II** was analyzed for percentage composition by weight of the following elements: C, H, N, and S. Based on the percentage composition by weight of N and S, the numbers of molecules of **I** and **II** per nanocrystal of silver were calculated to be 883 and 74, respectively.

(22) To obtain these values, the diameter of 170 silver nanocrystals modified by chemisorbed **II** were determined from a TEM image prepared by evaporation of a chloroformic dispersion of these nanocrystals on a carbon coated copper grid. It is noted that these nanocrystals clearly show long range ordering, an observation that strongly supports the assertion that these nanocrystals are relatively monodisperse.

(23) To obtain these values, a known weight of a sample silver nanocrystals modified by chemisorbed **II** was analyzed for percentage composition by weight of the following elements: C, H, N, and S. Based

on the percentage composition by weight of N, the number of molecules of **II** per nanocrystal of silver was calculated and found to be 1088.

(24) (a) Brienne, M.-J.; Gabard, J.; Lehn, J.-M. *J. Chem. Soc., Chem. Commun.* **1989**, 1868. (b) Cusack, L.; Rao, S. N.; Wenger, J.; Fitzmaurice, D. *Chem. Mater.* **1997**, *9*, 624. (c) Cusack, L.; Rao, S. N.; Fitzmaurice, D. *Chem. Eur. J.* **1997**, *3*, 202. (d) Cusack, L.; Marguerettaz, X.; Rao, S. N.; Wenger, J.; Fitzmaurice, D. *Chem. Mater.* **1997**, *9*, 1765.

(25) In this context we note that the chemical shifts observed initially might be due to changes in the acidity of the deuterated solvents used.

(26) Bellamy, L. J. *The Infrared Spectra of Complex Molecules*; Matheun: London, 1954.

(27) (a) Feibush, B.; Fiuroa, A.; Charles, R.; Onan, K.; Feibush, P.; Karger, B. *J. Am. Chem. Soc.* **1986**, *108*, 3310. (b) B. Feibush, M. Saha, Onan, K.; Karger, B.; Giese, R. *J. Am. Chem. Soc.* **1987**, *109*, 7531. (c) Hamilton, A.; Van Engen, D. *J. Am. Chem. Soc.* **1987**, *109*, 5035. (d) Bisson, A.; Carver, F.; Hunter, C.; Waltho, J. *J. Am. Chem. Soc.* **1994**, *116*, 10292.

(28) Pimentel, G.; McClellan, A. *The Hydrogen Bond*; Freeman: San Francisco, 1956.

(29) Family, F.; Landau, D., Eds. *Kinetics of Aggregation and Gelation*; North-Holland: Amsterdam, 1984.

(30) Weitz, D.; Huang, J.; Lin, M. Sung, J. *Phys. Rev. Lett.* **1985**, *54*, 1416.

(31) (a) Weitz, D.; Olivera, M. *Phys. Rev. Lett.* **1984**, *52*, 1433. (b) Weitz, D.; Huang, J.; Lin, M.; Sung, J. *Phys. Rev. Lett.* **1984**, *53*, 1657.

(32) Zhou, Z.; Chu, B. *J. Colloid Sci.* **1991**, *143*, 356. (b) Zhou, Z.; Wu, P.; Chu, B. *J. Colloid Sci.* **1991**, *146*, 541.